Journal of Atmospheric and Solar-Terrestrial Physics 73 (2011) 258–263

Contents lists available at ScienceDirect

Journal of Atmospheric and Solar-Terrestrial Physics

journal homepage: www.elsevier.com/locate/jastp

Global analysis of active longitudes of solar X-ray flares

L. Zhang [a,b,c], K. Mursula [a,*], I. Usoskin [d], H. Wang [b,c]

[a] University of Oulu, Department of Physics, Oulu, Finland
[b] National Astronomical Observatories, Chinese Academy of Sciences, Beijing, China
[c] Key Laboratory of Solar Activity, Chinese Academy of Sciences, Beijing, China
[d] University of Oulu, Sodankylä Geophysical Observatory, Oulu, Finland

ARTICLE INFO

Article history:
Accepted 7 December 2009
Available online 21 December 2009

Keywords:
Solar X-rays
Flares
Active longitudes

ABSTRACT

There is increasing evidence that various manifestations of solar activity are non-axisymmetric and mainly occur in two preferred longitude ranges, so called active longitudes. We have earlier analyzed the longitudinal occurrence of solar X-ray flares observed by GOES satellites using a specially developed dynamic, differentially rotating coordinate system. In this frame, the longitude distribution shows two persistent preferred longitudes separated by about 180 degrees whose strength alternates in time according to the so called flip-flop phenomenon. Here we make the first global statistical analysis to find the best fitting values for parameters describing the differential rotation of active longitudes of X-ray flares. We find that the new analysis greatly improves the earlier values for the rotation parameters, making them consistent between the three different classes of X-ray flares. The improved parameters also yield a systematically higher level of non-axisymmetry for the longitudinal distribution, thus increasing the statistical significance of the existence of active longitudes. Accordingly, a significant amount of X-ray flares of different classes are produced by the same two active longitudes. We also find a significant difference between the rotation rates in the two solar hemispheres, with active longitudes rotating faster than the Carrington rate in the northern hemisphere and slower than the Carrington rate in the southern hemisphere.

1. Introduction

It has been found that various manifestations of solar activity, such as sunspots (Bumba and Howard, 1965; Balthasar and Schüssler, 1984; Berdyugina and Usoskin, 2003), heliospheric magnetic fields (Ruzmaikin et al., 2001; Takalo and Mursula, 2002; Mursula and Hiltula, 2004) and flares (Bai and Cliver, 1990) are non-axisymmetric and mainly occur in preferred longitude ranges, so called active longitudes.

Using a specially developed dynamic, differentially rotating coordinate system, it was found (Usoskin et al., 2005) that two active longitudes of sunspots separated by about 180° have existed for the past 120 years. Recently, a similar dynamic system was used to analyze the longitudinal occurrence of solar X-ray flares observed by the NOAA/GOES satellites (Zhang et al., 2007a, b). In this frame, the longitude distribution of flares of different intensity showed two persistent preferred longitudes that were separated by about 180° and whose strength alternated in time similarly to the so called flip-flop phenomenon, which was first found in fast rotating cool stars (Jetsu et al., 1991) and later in the heliospheric magnetic field (Takalo and Mursula, 2002) and in sunspots (Berdyugina and Usoskin, 2003).

Sunspots and solar flares are different manifestations of solar magnetic fields, with sunspots being regions of the most intense photospheric fields and flares being related active regions and rapid changes in coronal magnetic fields. Since the rotation of photospheric and coronal structures is different, it is interesting to study the properties of active longitudes of both types of solar activity. When studying the first appearance of sunspots in a dynamic system it was found that such active longitudes, i.e., zones where sunspots preferentially first appear, are persistent for 120 years (Berdyugina and Usoskin, 2003; Usoskin et al., 2005). These longitudes can also be considered to be regions where strong magnetic fields are formed. Here we analyze longitudes of solar X-ray flares using a similar dynamic, differentially rotating coordinate system. The active longitudes of X-rays can be considered to be active and complex magnetic regions which experience fast changes.

In earlier studies the differential rotation parameters describing the dynamic system obtained for one solar activity variable such as one X-ray flare class were quite different from those obtained for another solar activity variable or another flare class (Zhang et al., 2007b). Moreover, a statistical analysis has so far been lacking to reliably evaluate whether the rotation parameters

* Corresponding author. Tel.: +358 8 5531366; fax: +358 8 5531287.
E-mail address: kalevi.mursula@oulu.fi (K. Mursula).

1364-6826/$ - see front matter © 2009 Elsevier Ltd. All rights reserved.
doi:10.1016/j.jastp.2009.12.003

obtained for any two sets of solar variables are in agreement or not.

Here we make an improved analysis of the GOES X-ray flare data in order to find, for the first time, the globally best fit values of parameters describing the differential rotation of active longitudes of solar X-ray flares. We also estimate the statistical errors of their best fit values for the first time. The paper is structured as follows. The data base is introduced in Section 2. The improved analysis is described in Section 3, and the best fit parameters are presented in Section 4. The difference between the rotation rates of the two solar hemispheres is discussed in Section 5, and the improved non-axisymmetry is depicted in Section 6. Finally, Section 7 presents our conclusions.

2. Data

We study here X-ray flares observed by the NOAA GOES satellites during the period of 1975–2006. Most of these X-ray flares were identified by simultaneous optical flare observations. The NGDC database (http://www.ngdc.noaa.gov/stp/SOLAR/ftpsolarflares.html#xray) provides the location information for the identified optical flares. We assume that the X-ray flares and optical flares are co-located and, using the central meridian distance of optical flares in this database, derive the Carrington longitudes of X-ray flare source regions.

X-ray flares are classified by their peak intensity. Table 1 shows the X-ray flare classes and the corresponding ranges of peak intensity. For convenience we sometimes call the C, M, and X-classes of X-ray flares the C-flares, M-flares and X-flares, respectively. During the study period of 1975–2006, there were altogether 23,393 C-flares, 4,426 M-flares, and 402 X-flares.

While the analysis of sunspots can be based on data extending over 120 years, for X-ray flares we only have three solar cycles of observations from the time when the GOES satellite series was initiated. We have not included here X-ray flare data in 2007 and 2008 since there were only few flares above C-class in these years.

3. Improved analysis

We treat in this work the migration of active longitudes with respect to the Carrington frame more accurately than earlier (Zhang et al., 2007b). This, together with the global search of optimum parameters, makes the obtained parameter values more reliable and consistent than in the earlier studies. We sketch the new approach below. For more information, we refer to the earlier studies (Usoskin et al., 2005; Zhang et al., 2007a, b).

On the k th day of the i th Carrington rotation, the migration M of an active longitude with respect to the Carrington reference frame is determined by

$$M = T_c \sum_{j=N_0}^{N_{i-1}} (\Omega_j - \Omega_c) + k(\Omega_{N_i} - \Omega_c) \quad (1)$$

where N_0 and N_{i-1} denote the numbers of the initial Carrington rotation and the $(i-1)$ th rotation, $T_c = 27.2753$ is the synodic Carrington rotation period and Ω_c is the angular rotation rate of Carrington system (in sidereal frame 14.1844 deg/day and in synodic frame 13.199 deg/day). Ω_{N_j} are the (sidereal) angular velocities of the active longitude during the j th Carrington rotation number N_j, which can be simply expressed by

$$\Omega_{N_j} = \Omega_0 - B \sin^2 \langle \phi_j \rangle, \quad (2)$$

where ϕ_j is the peak-intensity weighted average latitude of X-ray flares during this rotation (Zhang et al., 2007b). For Carrington rotations with no flare activity the linear interpolation of mean latitude is used. Ω_0, the (sidereal) equatorial angular frequency and B, the latitude variation parameter, are constants whose values will be determined by optimization.

Let us assume that one active longitude band is at longitude Λ_{ik1} on the k th day of the i th Carrington rotation, and at Λ_{01} at the beginning. Then, using the above migration, we obtain

$$\Lambda_{ik1} = (\Lambda_{01} + M) \bmod 360^\circ, \quad (3)$$

where mod 360° means modulo 360° within the range $[0^\circ, 360^\circ]$.

The other active longitude is assumed to be at $\Lambda_{ik2} = \Lambda_{ik1} \pm 180^\circ$, i.e., opposite to Λ_{ik1}. The difference between the longitudinal position of a flare, λ_{ik}, which occurred on the k th day of the i th rotation, and the center of the active longitude band, Λ_{ik1} or Λ_{ik2}, is defined as

$$\Delta_{ik} = \min(|\lambda_{ik} - \Lambda_{ik1}|, 360^\circ - |\lambda_{ik} - \Lambda_{ik1}|, |180^\circ - |\lambda_{ik} - \Lambda_{ik1}||). \quad (4)$$

In order to illustrate this, we discuss some examples. Assuming $\Lambda_{ik1} = 359^\circ$ and $\Lambda_{ik2} = 179^\circ$, and taking $\lambda_{ik} = 1^\circ$ one obtains $\Delta_{ik} = 360^\circ - |\lambda_{ik} - \Lambda_{ik1}| = 2^\circ$. On the other hand, taking $\lambda_{ik} = 177^\circ$, yields correspondingly $\Delta_{ik} = |180^\circ - |\lambda_{ik} - \Lambda_{ik1}|| = |\lambda_{ik} - \Lambda_{ik2}| = 2^\circ$. When $\lambda_{ik} = 357^\circ$, $\Delta_{ik} = |\lambda_{ik} - \Lambda_{ik1}| = 2^\circ$.

Note that earlier studies have missed the second term on the right-hand side of Eq. (1). So, the mean migration in a Carrington rotation (the first term on the right-hand side of Eq. (1)) was considered as the migration of active longitudes from the beginning to the end of the rotation. Here, fractional rotation of k days when the flare occurred is taken into account. The second term in Eq. (1) displays the migration of active longitudes during the k days of the i th rotation, from which we compute the longitude at flare occurrence, Λ_{ik1} in Eq. (3), rather than using the mean longitude of rotation Λ_{i1}, as was done in earlier studies. Finally, the more precise deviation Δ_{ik} in Eq. (4) is obtained by calculating $|\lambda_{ik} - \Lambda_{ik1}|$, rather than $|\lambda_{ik} - \Lambda_{i1}|$.

The mean deviation is defined as the average squared difference of flares from the nearest active longitude:

$$\varepsilon = \frac{1}{N} \sum_i \sum_k \Delta_{ik}^2, \quad (5)$$

where N is the total number of flares in the data set. Changing the value of Ω_0 in the interval [13.60, 15.0] (deg/day) with steps of 0.01, B within [0.0, 5.0] (deg/day) with steps of 0.01 and Λ_{01} within $[0^\circ, 360^\circ]$ with steps of 1°, the best fit parameters can be obtained when the least mean deviation is found. Thus, the mean deviation of Eq. (5) is used as the merit function of optimization. We note that this is effectively a two-parameter search since the third parameter Λ_{01} may have an arbitrary value related to the primary meridian, and is without any physical information. Applying the search method to every class of X-ray flares, we obtain the best fit parameters of differential rotation for the three X-ray flare classes (C-flares, M-flares, and X-flares), separately.

Table 1
X-ray flare classes and their ranges of peak intensities.

Class	W/m^2	ergs/cm^2/s
C	$10^{-6} \leqslant I \leqslant 10^{-5}$	$10^{-3} \leqslant I \leqslant 10^{-2}$
M	$10^{-5} \leqslant I \leqslant 10^{-4}$	$10^{-2} \leqslant I \leqslant 10^{-1}$
X	$I \geqslant 10^{-4}$	$I \geqslant 10^{-1}$

4. Differential rotation parameters

Scanning through the whole range of the three free parameters, we have found the globally best fit values for these parameters. Figs. 1, 2 and 3 depict the values of the mean

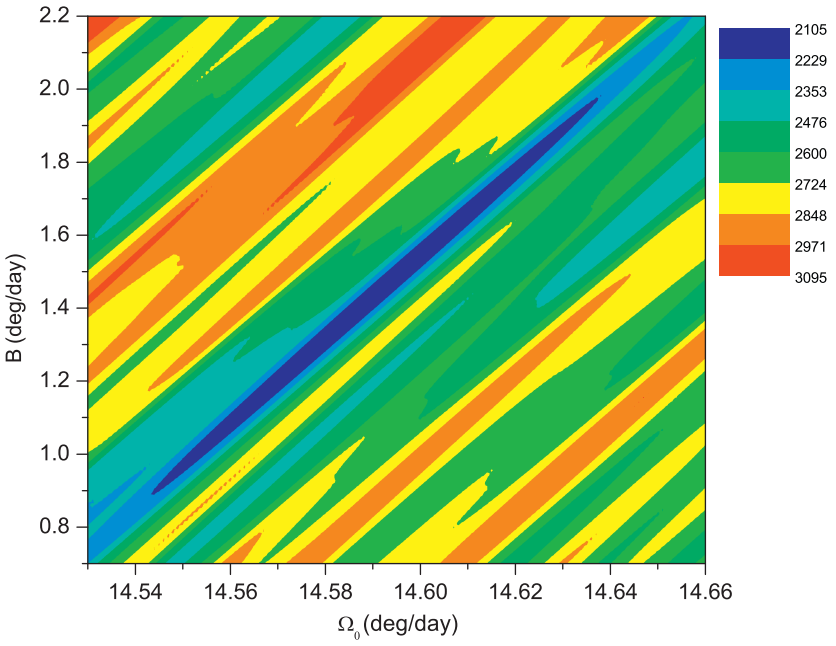

Fig. 1. Values of the mean deviation ε (the merit function of optimization) in grey scaling (color coding in web color version) as a function of Ω_0 and B for C-class flares of the northern hemisphere. Only the region around the best fit parameter values are shown.

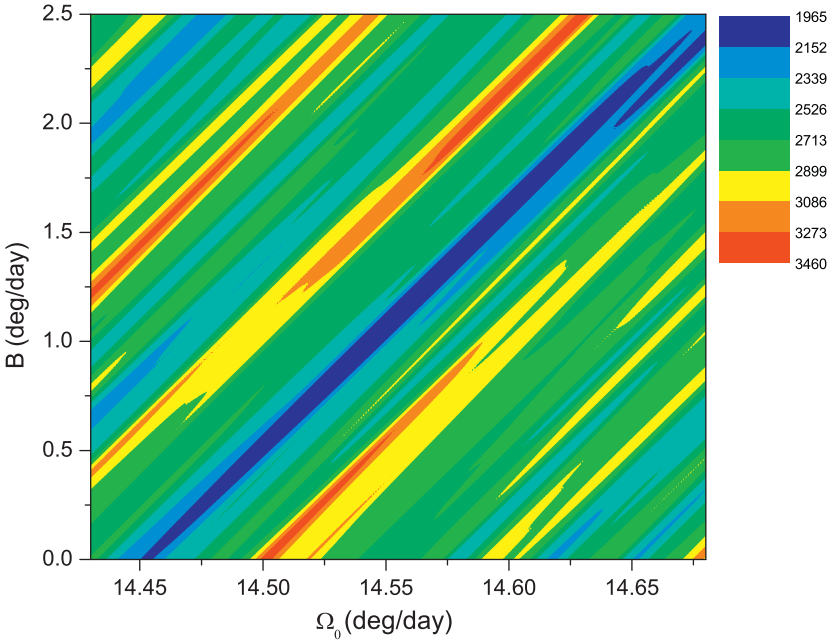

Fig. 2. The same as Fig. 1 but for M-class flares of the northern hemisphere.

deviation ε in black and white coding (color coding in web color figures) around the deepest (global) minimum, i.e. around the best fit values of the Ω_0 and B parameters for the C, M and X-flares in the northern hemisphere. (Note that Figs. 1, 2 and 3 show only a part of the full studied parameter range). The best fit values are found at the center of an elongated area of small values of ε, and their errors denote the horizontal and vertical extent of this area, respectively. E.g., from Fig. 1 one can extract the best fit value and error for $\Omega_0 = 14.59 \pm 0.04$ (deg/day) and $B = 1.43 \pm 0.5$ (deg/day) for the northern C-class flares. Figs. 1, 2 and 3 also show that, in agreement with the errors depicted in Table 2, the best fit parameter area increases from C-flares to M-flares and is largest for X-class flares. This is due to the smaller number of M-class flares and, in particular, of X-class flares which leads to smaller statistics.

The best fit values of Ω_0 and B are listed in Table 2 for the three X-ray flare classes separately for the northern and southern hemispheres. In order to compare the new results with the earlier, we list the best fit parameters obtained earlier (Zhang et al., 2007b) in Table 3. Comparing Tables 2 and 3, one can see that the

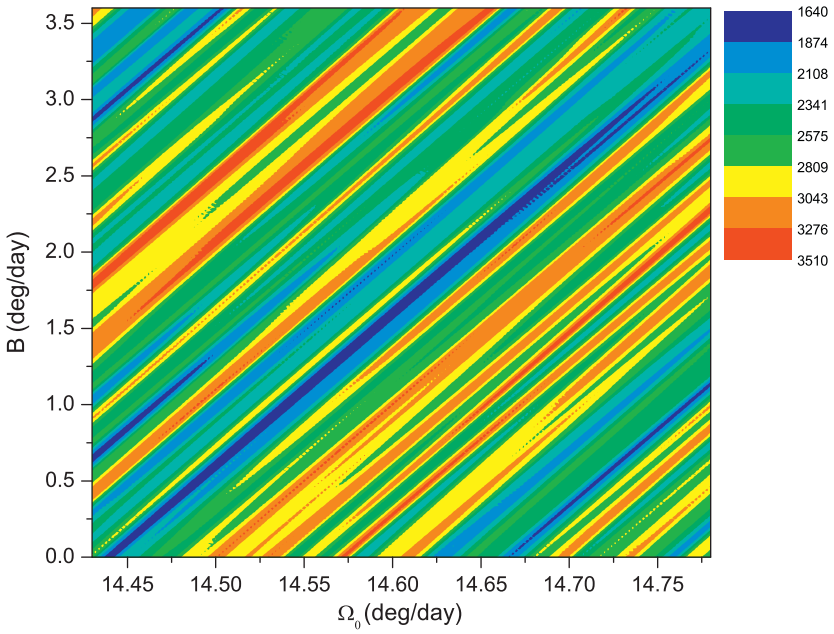

Fig. 3. The same as Fig. 1 but for X-class flares of the northern hemisphere.

Table 2
The best fit values of differential rotation parameters Ω_0 and B determined for the three X-ray flare classes for northern and southern hemispheres separately.

	Northern		Southern	
	Ω_0 (deg/day)	B (deg/day)	Ω_0 (deg/day)	B (deg/day)
C-flares	14.59 ± 0.04	1.43 ± 0.50	14.39 ± 0.04	2.80 ± 0.50
M-flares	14.60 ± 0.10	1.62 ± 1.20	14.42 ± 0.08	3.32 ± 0.80
X-flares	14.60 ± 0.15	1.76 ± 1.50	14.49 ± 0.12	3.87 ± 1.30

Table 3
The same as Table 2 but for best fit values obtained earlier (Zhang et al., 2007b).

	Northern		Southern	
	Ω_0	B	Ω_0	B
C-flares	14.81	3.91	13.79	3.47
M-flares	14.59	3.53	14.33	1.55
X-flares	14.93	3.50	14.50	3.93

new best fit values of the two parameters for the three flare classes in either hemisphere are more similar to each other than earlier. E.g., the values of Ω_0 for C, M and X-flares in the northern hemisphere all agree to within 0.01 (deg/day) while, earlier, their maximum difference was as large as 0.34 (the difference between M-flares and X-flares).

Although the spread of the Ω_0 values in the southern hemisphere is somewhat wider (0.1 deg/day) than in the northern hemisphere, it is greatly reduced in comparison to the earlier results (0.71 deg/day). Moreover, the new best fit values of Ω_0 and B for the three flare classes all agree with each other within the estimated errors. No similar analysis was made earlier for X-ray flares but, using the newly obtained errors, the earlier three values would differ from each other by several standard deviations. Accordingly, the best fit values of the two differential rotation parameters determined by new analysis are more consistent than earlier.

Note that the elongated areas in Figs. 1, 2 and 3 show that Ω_0 and B are strongly correlated. Accordingly, independent errors of these two parameters are even considerably (typically an order of magnitude) smaller than the correlated errors depicted in Table 2.

Let us now calculate the (sidereal) angular frequency Ω_{N_i} at the mean latitude. Note that the correlation between Ω_0 and B also tends to reduce the differences in angular velocity Ω_{N_i} between the three flare classes in either hemisphere. In fact, using the average flare latitude of 17°, the northern C-class flares have the angular frequency $\Omega_{N_i} = 14.468 \pm 0.002$ (deg/day). Correspondingly, $\Omega_{N_i} = 14.462 \pm 0.006$ (deg/day) for northern M-flares and 14.450 ± 0.021 (deg/day) for northern X-flares. Thus the maximum difference in Ω_{N_i} between the three flare classes is 0.018 deg/day which is within the error bars. The fact that the best fit parameter values, and in particular, the derived Ω_{N_i} values are so similar for the three flare classes with so different statistics, gives additional support of the new method.

5. North–south asymmetry

Fig. 4 shows the best fit parameter range for the C-class flares of the southern hemisphere. As shown in Table 2, in the southern hemisphere the best fit values for Ω_0 and B differ between the three X-flare classes more from each other than in the north. Therefore, the effect of the above discussed strong correlation between the Ω_0 and B becomes more notable in the south. The obtained angular velocities Ω_{N_i} in the south at the mean latitude 17° are 14.151 ± 0.002 (deg/day) for C-flares, 14.136 ± 0.005 (deg/day) for M-flares, and 14.159 ± 0.021 (deg/day) for X-flares. Accordingly, the largest difference is only 0.023 (deg/day) which is within the error bars, similarly as in the northern hemisphere. The fact that the best fit parameter values, and in particular, the derived Ω_{N_i} values are so similar for the three flare classes with so different statistics, gives strong support of the new method.

Note also that, as suggested by the different best fit values for Ω_0 and B for the two hemispheres (see Table 2), the angular velocities Ω_{N_i} of active longitudes are also different for the northern (about 14.468 deg/day) and southern (about

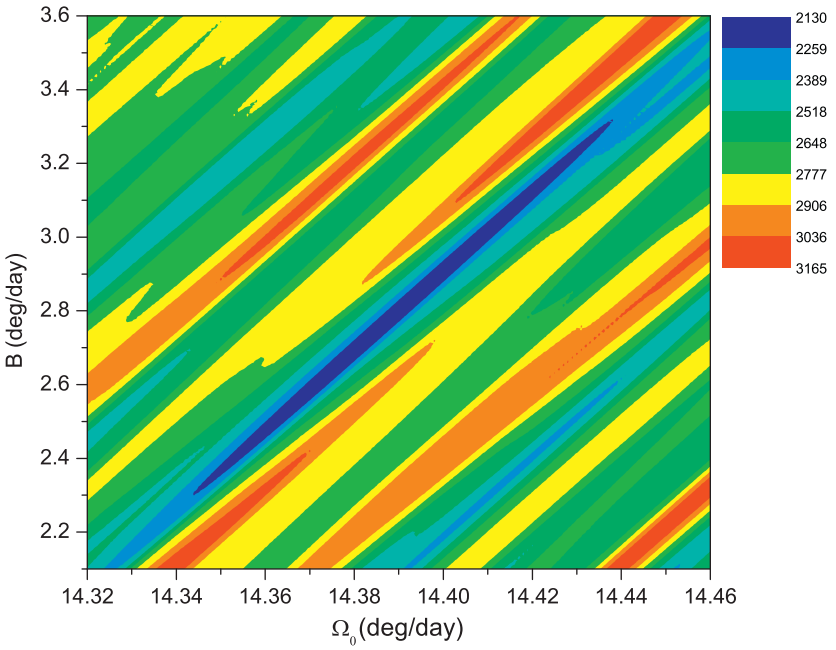

Fig. 4. The same as Fig. 1 but for C-class flares of the southern hemisphere.

14.151 deg/day) hemispheres. This difference is statistically significant (by more than 10 standard deviations), and indicates that, at least during the interval studied here, the active longitudes in the northern hemisphere rotate, on an average, faster than the southern hemisphere. Note also that, interestingly, the northern hemisphere rotates faster than the Carrington rotation rate and the southern hemisphere slightly slower than that. The corresponding sidereal and synodic rotation periods are 24.88 days and 26.71 days for the north and 25.44 days and 27.35 days for the south.

6. Quantifying non-axisymmetry

We define the measure of non-axisymmetry Γ in the same as earlier:

$$\Gamma = \frac{N_1 - N_2}{N_1 + N_2}, \tag{6}$$

where N_1 and N_2 denote the number of flares occurring within and outside of the two active longitude taken here as two 90° wide bands as follows:

$$N_1 = \sum_{k,i} 1 \text{ if } (|\lambda_{ik} - \Lambda_{ik}| < 45^\circ \text{ or } 360^\circ - |\lambda_{ik} - \Lambda_{ik}| < 45^\circ), \tag{7}$$

$$N_2 = \sum_{k,i} 1 \text{ if } (|\lambda_{ik} - \Lambda_{ik}| > 45^\circ \text{ and } 360^\circ - |\lambda_{ik} - \Lambda_{ik}| > 45^\circ). \tag{8}$$

We have depicted the non-axisymmetry parameters Γ and the related percentages of the three X-ray flare classes that occurred within the active longitudes, i.e., the ratios $N_1/(N_1+N_2)$ in Table 4. For comparison with these new results, the earlier values for the same parameters are shown in Table 5. Northern and southern hemispheres are treated separately, as above. One can see in Tables 4 and 5 that the new, improved analysis method has increased the non-axisymmetry of active longitudes in all three X-ray classes and for both hemispheres. This is another demonstration of the fact that the new method indeed can disclose the actual, non-asymmetric situation better than the earlier method. It is also interesting to note that, despite the hemispheric difference in rotation rate, the amount of non-asymmetry is very similar in the two hemispheres. The new method yields also here a slightly more similar and consistent result. The non-asymmetry parameters increase with X-ray flare class in both hemispheres, confirming that stronger manifestations of solar activity tend to concentrate more to active longitudes (Zhang et al., 2007a, b). Non-axisymmetry increases gradually from 0.20 to 0.24 for C-flares to 0.58–0.59 for X-flares, which implies that nearly 80% of X-flares originated at the active longitudes during the last three solar cycles. This gives interesting possibilities for improved prediction of flares and other space weather events (Zhang et al., 2008).

Non-axisymmetry in dynamo models has been studied in many papers. Both non-axisymmetric (Rüdiger and Elstner, 1994; Bigazzi and Ruzmaikin, 2004; Rüdiger et al., 2003) and axisymmetric (Stix, 1971; Ivanova and Ruzmaikin, 1971; Moss, 1999, 2005) dynamo models can excite non-axisymmetric magnetic

Table 4
Non-axisymmetry parameters for three X-ray flare classes in the two hemispheres.

	North		South	
	Γ	$N_1/(N_1+N_2)$	Γ	$N_1/(N_1+N_2)$
C-flares	0.24 ± 0.02	$62\% \pm 1\%$	0.20 ± 0.03	$60\% \pm 2\%$
M-flares	0.32 ± 0.04	$66\% \pm 2\%$	0.27 ± 0.01	$64\% \pm 1\%$
X-flares	0.58 ± 0.05	$79\% \pm 3\%$	0.59 ± 0.10	$79\% \pm 5\%$

Table 5
The same parameters as in Table 4 but according to earlier calculations Zhang et al. (2007b).

	North		South	
	Γ	$N_1/(N_1+N_2)$ (%)	Γ	$N_1/(N_1+N_2)$ (%)
C-flares	0.15	58	0.14	57
M-flares	0.27	63	0.20	60
X-flares	0.55	78	0.49	74

fields. Another alternative to explain the active longitudes is a non-axisymmetric magnetic structure which is affected by differential rotation but still rotating quasi-rigidly (Berdyugina et al., 2006). However, despite these developments more work is still needed to solve the problem.

7. Conclusions

We have made here a corrected, global analysis to find the best fit values of parameters describing the rotation of the active longitudes producing solar X-fay flares. The global analysis yields parameter values that are highly consistent for the different flare classes. The best fit values of Ω_0 parameters for C, M and X-flares agree within 0.01 deg/day in the northern hemisphere and within 0.10 deg/day in the south. Moreover, the three X-ray classes depict angular frequencies that are closely similar to each other (within 0.01 deg/day in the northern hemisphere and 0.02 deg/day in the south), the difference being within the error bars. Accordingly, we found for the first time that active longitudes having the same rotation rates are responsible for all the three X-ray flare classes. This gives strong support for the success of the improved method and the extracted parameter values. Moreover, the improved parameters yield a higher level of non-axisymmetry for the longitudinal distribution, thus increasing evidence for the existence of active longitudes.

Interestingly, we also found that the active longitudes rotate at significantly different average angular frequencies in the two hemispheres. Using the mean flare latitude of about 17°, we found that the sidereal and synodic rotation periods are 24.88 ± 0.01 days and 26.71 ± 0.01 days in the north and 25.44 ± 0.01 days and 27.35 ± 0.01 days in the south. Thus, the active longitudes in the north rotate significantly faster than the Carrington rate and in the south slightly slower than that.

Finally, we note that the existence of persistent active longitudes can also help us to understand more about how solar activity affects the interplanetary environment. In the future, it will also allow to make better forecasts of, e.g., magnetic storms and geomagnetic activity. It is also clear that persistent existence of active longitudes and their north-south asymmetric rotation provides interesting observational constraints upon realistic solar dynamo models.

Acknowledgments

The research leading to these results has received funding from the European Commission's Seventh Framework Programme (FP7/2007-2013) under the Grant agreement no. 218816 (SOTERIA Project, http://www.soteria-space.eu). We also acknowledge the financial support by the Academy of Finland to the HISSI research project no. 128189. This work is jointly supported by the National Basic Research Program of China (Program 973) through Grant 2006CB806307, the National Natural Science Foundation of China (NSFC) through Grants 10673017, 10733020, 10803011 and 40890161, and Projects KJCX2-YW-T04 and KGCX3-SYW-403C10 of the Chinese Academy of Sciences (CAS).

References

Bai, T., Cliver, E.W., 1990. A 154 day periodicity in the occurrence rate of proton flares. Astrophys. J. 363, 299–309.
Balthasar, H., Schüssler, M., 1984. Evidence for the 22-year-cycle in the longitudinal distribution of sunspots. Solar Phys. 93, 177–179.
Berdyugina, S.V., Usoskin, I.G., 2003. Active longitudes in sunspot activity: century scale persistence. Astron. Astrophys. 405, 1121–1128.
Berdyugina, S.V., Moss, D., Sokoloff, D., Usoskin, I.G., 2006. Active longitudes, nonaxisymmetric dynamos and phase mixing. Astron. Astrophys. 445, 703–714.
Bigazzi, A., Ruzmaikin, A., 2004. The sun's preferred longitudes and the coupling of magnetic dynamo modes. Astrophys. J. 604, 944–959.
Bumba, V., Howard, R., 1965. A study of the development of active regions on the sun. Astrophys. J. 141, 1492–1501.
Ivanova, T.S., Ruzmaikin, A.A., 1971. Three dimensional model for generation of the mean solar magnetic field. Astron. Nachr. 306, 177–186.
Jetsu, L., Pelt, J., Tuominen, I., Nations, H., 1991. The spot activity of FK Comae Berenices. In: Tuominen, I., Moss, D., Rüdiger, G. (Eds.), IAU Colloquium 130: The Sun and Cool Stars. Activity, Magnetism, Dynamos. Lecture Notes in Physics, vol. 380. Springer, Berlin, pp. 381–383.
Moss, D., 1999. Non-axisymmetric solar magnetic fields. Mon. Not. R. Astron. Soc. 306, 33–306.
Moss, D., 2005. Nonaxisymmetric magnetic field generation in rapidly rotating late-type stars. Astron. Astrophys. 432, 249–259.
Mursula, K., Hiltula, T., 2004. Systematically asymmetric heliospheric magnetic field: evidence for a quadrupole mode and non-axisymmetry with polarity flip-flops. Solar Phys. 224, 133–143.
Rüdiger, G., Elstner, D., 1994. Non-axisymmetry vs. axisymmetry in dynamo-excited stellar magnetic fields. Astron. Astrophys. 281, 46–50.
Rüdiger, G., Elstner, D., Ossendrijver, M., 2003. Do spherical α^2- dynamo oscillate? Astron. Astrophys. 406, 15–21.
Ruzmaikin, A., Feynman, J., Neugebauer, M., Smith, E.J., 2001. Preferred solar longitudes with signatures in the solar wind. J. Geophys. Res. 106, 8363–8370.
Stix, M., 1971. A non-axisymmetric $\alpha-$effect dynamo. Astron. Astrophys. 13, 203–208.
Takalo, J., Mursula, K., 2002. Annual and solar rotation periodicities in IMF components: evidence for phase/frequency modulation. Geophys. Res. Lett. 29 (9), 1317 (CiteID).
Usoskin, I.G., Berdyugina, S.V., Poutanen, J., 2005. Preferred sunspot longitudes: non-axisymmetry and differential rotation. Astron. Astrophys. 441, 347–352.
Zhang, L.Y., Cui, Y.M., He, Y.L., He, H., Du, Z.L., Li, R., Wang, H.N., 2007a. Longitudinal distribution of major solar flares during 1975–2005. Adv. Space Res. 40, 970–975.
Zhang, L.Y., Wang, H.N., Du, Z.L., Cui, Y.M., He, H., 2007b. Long-term behavior of active longitudes for solar X-ray flares. Astron. Astrophys. 471, 711–716.
Zhang, L.Y., Wang, H.N., Du, Z.L., 2008. Prediction of solar active longitudes. Astron. Astrophys. 484, 523–527.